Electrochemistry Communications 103 (2019) 109–113

Contents lists available at ScienceDirect

Electrochemistry Communications

journal homepage: www.elsevier.com/locate/elecom

Enabling fast charging of high energy density Li-ion cells with high lithium ion transport electrolytes

Zhijia Du*, David L. Wood III, Ilias Belharouak

Energy and Transportation Science Division, Oak Ridge National Laboratory, One Bethel Valley Rd, Oak Ridge, TN 37830, United States of America

ARTICLE INFO

Keywords:
Fast charging
NMC811
Electrolyte
LiFSI

ABSTRACT

Enabling fast charging capability of high energy density Li-ion cells could dramatically increase the widespread adoption of battery electric vehicles. However, fast charging is limited by Li ion depletion in the electrolyte and increasing Li ion transport from cathode to anode is essential. By evaluating different Li salts in the electrolyte, we find lithium bis(fluorosulfonyl)imide (LFSI) has both higher conductivity and higher Li ion transference number compared to the traditional $LiPF_6$ salt. In a 12-minute charge, the electrolyte with $LiPF_6$ salt reaches the cut-off voltage rapidly while the one with LiFSI exhibits a longer constant current charge with more capacity achieved. The LiFSI electrolyte also shows better cycling performance and less Li plating after repeated fast charging cycles.

1. Introduction

Energy density, cost and safety are, more than ever, the most significant barriers to overcome in order to increase the wide acceptance of Li-ion batteries (LIBs) in electric vehicles (EVs) [1]. The U.S. Department of Energy (DOE) has set ultimate goals for battery electric vehicles (BEVs), which include reducing the production cost of the battery pack to $150/kWh, increasing the electrical range of the battery to 300 miles, and decreasing the charging time to 15 min or less [2]. Increasing electrode thickness, and hence increasing active material loading, is an effective way to achieve these energy density and cost targets [3]. The caveat, however, is that thicker electrodes fail during fast charging.

The relationship between battery energy density, power density and areal capacity in thick electrodes has been studied by Du et al. [3] and Gallagher et al. [4]. The results suggested that the rate capability is limited by both the Li-ions mass transport in liquid electrolytes and interfacial overpotential in graphite anodes [4,5]. The findings also implied that a significant portion of the available energy in thick electrodes cannot be accessed because of the depletion of Li-ions in the electrolyte phase [3]. On the battery design side, Ahmed et al. suggested that the electrodes need to be thinner than the typical 40–60 μm should fast charging be one of the requirements for EVs [5]. Nonetheless, current Li-ion battery chemistries using thin electrodes stand no chance for meeting the requisites of extended electrical drive range and cost despite the power advantage.

One of the major issues in battery extreme fast charging (XFC) is the plating of lithium metal over graphite anodes due to sluggish kinetics. This phenomenon was pointed out as a major reason for cell performance degradation and failure in a recent battery technology gap analysis [2,4]. The worst aspect of plating is the dendritic growth of metallic lithium which would not only restrict reversible Li-ions inventory but also jeopardize the cell safety through shorting [6,7]. This was correlated with the depletion of Li-ions in the electrolyte as modeled by Chazalviel's et al. [8], and demonstrated by others research groups [9–11]. Indeed, Hwang et al. found by an operando transmission X-ray microscopy study that the growth of the dendritic forms of lithium metal was significantly enhanced as result of the lack of Li-ions in electrolyte phase near graphite electrode [10].

One of the solutions for enabling extreme fast charging while retaining most of the battery energy can be achieved through the significant enhancement of the Li-ion mass-transport in electrolytes such that enough Li ions are available for intercalation in graphite. The mass transport of Li ions can be evaluated by two macroscopic characteristic values: 1) the Li ion conductivity, which is related to the total flux of charge carriers, 2) the Li ion transference number, which is related to the fraction of the total current carried by Li ions. An electrolyte with both higher Li ion conductivity and transference number is ideal for higher Li ion transport and would be a significant step towards realizing cells with high charging rates. The present study deals with the evaluation of the salt, lithium bis(fluorosulfonyl)amide (LiFSI) [12–16], as a potential alternative candidate for the salt, lithium

* Corresponding author.
E-mail address: duz1@ornl.gov (Z. Du).

https://doi.org/10.1016/j.elecom.2019.04.013
Received 23 January 2019; Received in revised form 29 April 2019; Accepted 30 April 2019
Available online 01 May 2019

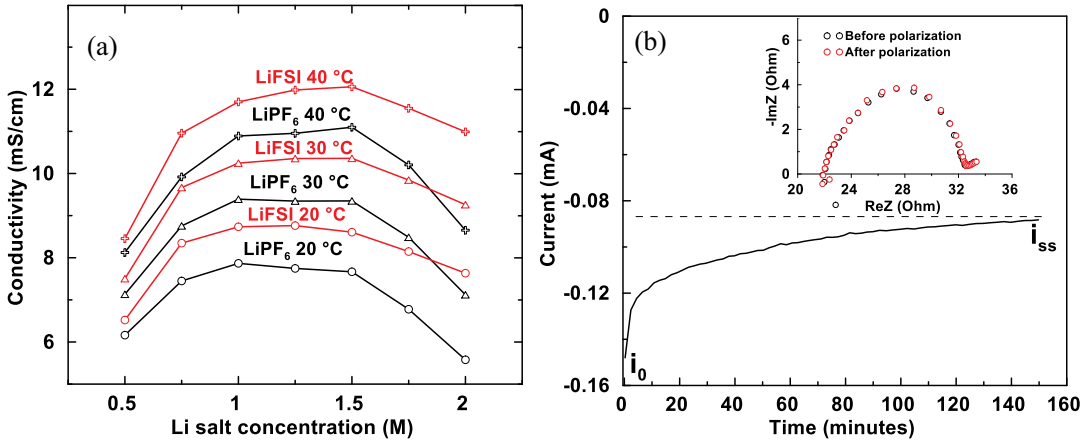

Fig. 1. (a) Conductivity of LiFSI and $LiPF_6$ in (EC:EMC) (30:70 wt%) as function of concentration and temperature. (b) Chronoamperogram of 1.5 M LiFSI in EC:EMC (30:70 wt%) with an applied voltage of 5 mV and the inset is Nyquist plot before and after the polarization experiment.

hexafluorophosphate ($LiPF_6$), in cells designed for fast charging. The study sheds the light on the higher Li ion conductivity and transference number in electrolytes comprising the salt LiFSI.

2. Experimental

$LiNi_{0.8}Mn_{0.1}Co_{0.1}O_2$ (NMC811) and graphite electrodes were fabricated at the US. Department of Energy (DOE) Battery Manufacturing R&D Facility (BMF) at Oak Ridge National Laboratory [17]. The positive electrode composition was 90 wt% NMC811 (Targray), 5 wt% carbon black (Denka Li-100) and 5 wt% polyvinylidene fluoride (PVDF, Solvay 5130). The areal loading of the electrode was 14.1 mg/cm^2 (2.35 mAh/cm^2) after calendaring to 30% porosity. The negative electrode composition was 92 wt% graphite (Superior Graphite1520T), 2 wt% carbon black (Timical C65) and 6 wt% polyvinylidene fluoride (PVDF, Kureha 9300). The areal loading was 8.0 mg/cm^2 (2.6 mAh/cm^2) after calendaring to 30% porosity.

The electrolytes were made of 1.5 M lithium salts dissolved in a combination of ethylene carbonate (EC) and ethyl methyl carbonate (EMC) (30:70 wt%). The lithium salts were $LiPF_6$ (Sigma-Aldrich, purity ≥ 99.99%) and LiFSI (HSC corporation, purity ≥ 99.95%).

The pouch cells were assembled with one layer of anode, one layer of cathode and one layer of separator (Celgard 2325). The cells were vacuum filled with the electrolytes. Cell assembly was carried out inside a dry room with a dew point of less than −50 °C and relative humidity (RH) of 0.1% at BMF. The cells were cycled between 2.5 and 4.2 V using the battery cycler, Maccor Series 4000, coupled with an environmental chamber set at 30 °C. For the charging protocols, the current was calculated from the nominal capacity, and the charging step was ended in 60, 30, 20, and 12 min (1C (185 mA/g_{NMC811}), 2C (370 mA/g_{NMC811}), 3C (555 mA/g_{NMC811}), and 5C (925 mA/g $_{NMC811}$), respectively). The cells were charged under constant current to the upper cutoff voltage of 4.2 V and held there until the respective time limit was reached. Three cell replicates were fabricated and tested to ensure reproducibility.

Conductivity measurements of the electrolyte were carried out using a conductivity cell (Cole-Parmer). The conductivity cell was calibrated using standard KCl solutions. The conductivities were measured using electrochemical impedance spectroscopy from 10 Hz to 1 MHz with a 6 mV perturbation voltage using a potentiostat (Bio-Logic). As for transference number measurement, we used an electrochemical method similar to previous reports [18,19]. In essence, a nonblocking cell was assembled using a revised conflat cell [20] with two stainless steel (SS) spacers as current collectors in close contact with two lithium metal disks sandwiching a high-density polyethylene cylinder. The cylinder was filled with the electrolytes, and the distance between the two lithium disks was 8 mm. A voltage bias of 5 mV was applied during the potentiostatic polarization experiments, and the impedances were measured in the frequency range of 1–100 kHz with a 5 mV perturbation voltage using a Bio-Logic potentiostat.

3. Results and discussion

Fig. 1 shows the conductivity of electrolytes, measured at 20, 30 and 40 °C, as a function of $LiPF_6$ or LiFSI concentrations in the solvent system (EC:EMC) (30:70 wt%). With the increase of concentrations of the lithium salts from 0.5 to 1 M, the conductivity increased due to the increased number of dissociated ions in the electrolyte solutions. With further increase of the salt concentrations, the cationic and anionic species form pairs and hence do not contribute to conductivity, in agreement with other reports [21]. In our case, the conductivity reached topmost values in the range of 1–1.5 M, and then decreased thereafter. With the increase of temperature, the maximal conductivity values shifted from 1 M at 20 °C to 1.5 M at 40 °C, owing to higher thermal agitation that increases the dissociation of ion pairs. When comparing the two lithium salts, LiFSI consistently shows a higher conductivity compared to $LiPF_6$ under the same concentration and temperature (Table S1). For example, the conductivity of LiFSI is 10.36 mS/cm compared to 9.35 mS/cm of $LiPF_6$ at the same 1.5 M concentration and same temperature 30 °C. This finding is in agreement with a previous report ascribing the higher conductivity to a higher degree of dissociation of LiFSI [22]. Another interesting finding is that the conductivity drop for LiFSI from 1.5 to 2.0 M concentrations was less severe than for $LiPF_6$, which is expected to ease the electrolyte depletion issue when fast charging and discharging is applied to Li-ion cells [3].

The lithium-ion transference number (t_+), that is another important electrolyte feature, is expressed by the following equation [23]:

$$t_+ = \frac{I_{ss}(\Delta V - I_0 R_0)}{I_0(\Delta V - I_{ss} R_{ss})} \quad (1)$$

where I_{ss} is the steady-state current, I_0 is the initial current, ΔV is the applied potential, and R_0 and R_{ss} are the electrode resistances before and after polarization, respectively. The electrolyte with the $LiPF_6$ salt has a t_+ of 0.382 (Fig. S1), which is within the range of 0.24 to 0.39 as reported by others [18,19], and the t_+ of the LiFSI based electrolyte measured in this study is 0.495. Our hypothesis is that both the higher dissociation of the LiFSI salt in the electrolyte and the larger size of the FSI^- anion contribute to the transference number enhancement. The higher dissociation indicates that Li ions can move more freely due to less attractive forces by the anions. The larger size of FSI^- (95 Å^3 [22]) compared to PF_6^- (69 Å^3) suggests slower movement of FSI^-, and as a result, Li-ions are able to move faster in the presence of the FSI^- ions.

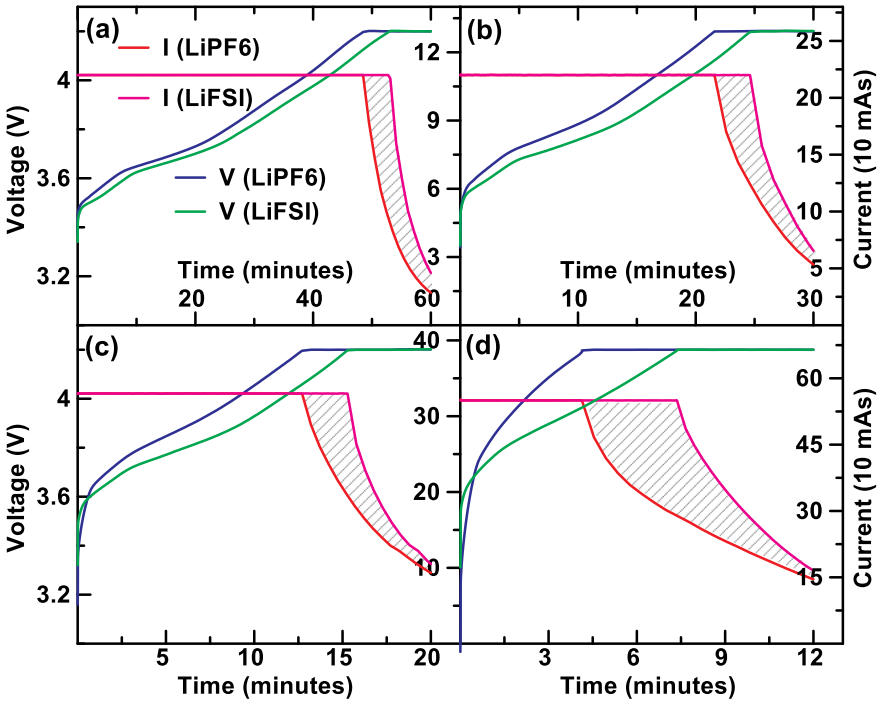

Fig. 2. Voltage (V) and Current (I) versus charging time for cells charged at (a) 1C, (b) 2C, (c) 3C and (d) 5C, with time cut-off of 1 h, 30 min, 20 min and 12 min, respectively. The voltage (V) curves correspond to the y-axis on the far left while the current (I) curves correspond to the y-axis on the right of each corresponding panel.

The higher Li ion transference number in LiFSI compared to the $LiPF_6$ case is also in accordance with previous report [12].

Fig. 2 shows the fast charging capability of the cell comprising $LiNi_{0.8}Mn_{0.1}Co_{0.1}O_2$ (NMC811) as the cathode and graphite as the anode and in the presence of the LiFSI and $LiPF_6$ based electrolytes. Under the 1C rate (Fig. 2a), the cell voltages gradually increased during the constant current (CC) charging and reached the cut-off voltage (4.2 V) around 49.5 min ($LiPF_6$) and 53.1 min (LiFSI). The cells were further charged under the constant voltage (CV) mode with a decreasing trickle current till the overall charging reached 60 min. With increasing the charge current to 2C (Fig. 2a) and 3C (Fig. 2a), the cells with the $LiPF_6$ electrolyte attained the cut-off voltage earlier than the ones with the LiFSI electrolyte. This gap widened even further under a 5C charge as shown in Fig. 2d. In this case, the cell with the $LiPF_6$ electrolyte had only 4.2 min under the CC charge while the one with the LiFSI electrolyte had 7.4 min under the CC charge. This large gap (shaded areas in Fig. 2), between the plots of the current (I) vs. time, indicates that more capacity can be stored when the cell has a longer CC charging time under the intended C-rate.

Fig. 3 shows the corresponding discharge voltage curves at the C/2 rate for the cells charged under 1C, 2C, 3C and 5C rate as shown in Fig. 2. When the cells were charged in 1 h, they delivered 173.8 and 170.8 mAh/g capacity in the presence of the LiFSI and $LiPF_6$ electrolyte, respectively. The capacity difference grew further when the charge rate was increased to 5C and charging time shortened to 12 min. The cell with the LiFSI electrolyte had a capacity of 153.2 mAh/g, which is a 13% improvement over the $LiPF_6$ electrolyte (i.e. 135.4 mAh/g).

Fig. 4 shows the cycling performance of under 12-minute fast charging through 500 cycles. The cell with the LiFSI electrolyte exhibited minimal capacity fading over the 500 cycles with 134.3 mAh/g capacity retained (84% retention compared to 1st cycle of 12-minute

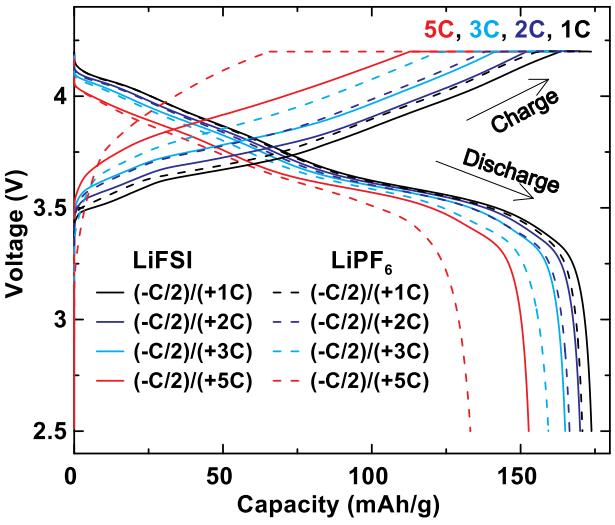

Fig. 3. Charge (different C rate) and discharge voltage curves (all at C/2) of NMC811/graphite cells with $LiPF_6$ and LiFSI electrolyte.

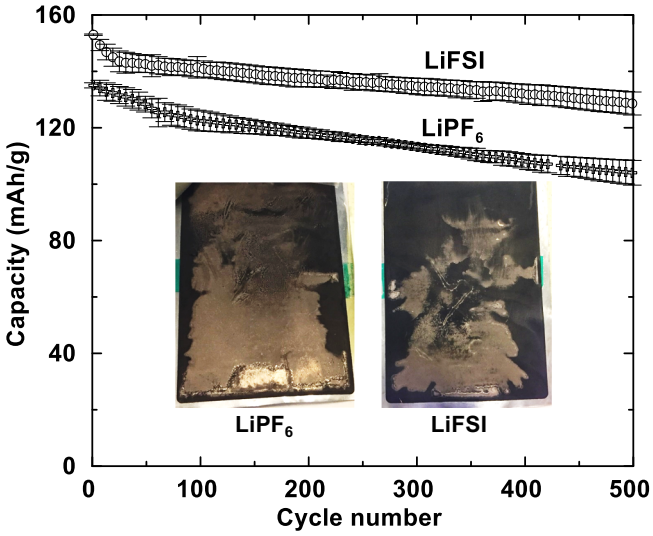

Fig. 4. Long term cycling performance of the cells with LiFSI and $LiPF_6$ electrolytes with 12 minute fast charging. Inserted photos show the extent of Li plating on each graphite electrode.

Table 1
BatPac cell parameters in 60 Ah pouch cells when different electrolytes are used.

Salt in electrolyte	Charging time (minutes)	Capacity (mAh/g)	Voltage (V)	Cell energy (Wh)	Gravimetric energy density (Wh/kg)	Volumetric energy density (Wh/L)
LiFSI	60	173.8	3.69	220.58	212.51	497.93
	30	170.0	3.68	215.15	207.27	485.66
	20	165.0	3.67	208.23	200.61	470.04
	12[a]	153.2	3.64	191.67	184.66	432.67
	12[b]	134.3	3.64	167.93	161.78	379.08
$LiPF_6$	60	170.8	3.69	220.58	210.08	493.48
	30	166.5	3.68	210.30	200.29	470.47
	20	159.4	3.66	200.18	190.65	447.84
	12[a]	135.4	3.62	168.39	160.37	376.71
	12[b]	110.6	3.67	139.40	132.76	311.85

[a] The first cycle using 12 minute charge.
[b] The 500th cycle using 12 minute charge.

charge). The cell with $LiPF_6$ electrolyte showed rapid capacity fading during the first 100 cycles and then decreased steadily with further cycling. This cell only had 110.6 mAh/g capacity retained (77% retention) after 500 cycles. The cells after 500 cycles were opened inside an Ar-filled glove box after discharging to 2.0 V for observation. Both cells showed lithium platting after repeated fast charging cycles. However, the lithium plating area on the graphite electrode was much smaller for the LiFSI electrolyte compared to the $LiPF_6$ electrolyte, which is ascribed to the better Li-ion transport properties of the LiFSI based electrolyte compared to the $LiPF_6$ one. No corrosion of the cathode Al current collector was observed after 500 cycles for the cell with LiFSI electrolyte. It has been reported that Al corrosion can be greatly suppressed by eliminating chloride impurity [13]. The free chloride in the LiFSI in this study was only 1 ppm, which virtually eliminated any Al corrosion.

To evaluate the cells for automotive applications, we used the electrode and cell design BatPac model [24], and the summary is shown in Table 1. The cathode thickness was set at 55 μm and the pouch cell had a capacity of 60 Ah. The cell mass/volume ratio was 1.038 kg/443 mL for the LiFSI electrolyte cell, while the mass/volume ratio was 1.050 kg/447 mL for the $LiPF_6$ electrolyte cell. Based on the above experimental results, for a 1-hour charge, the cells with the two different electrolytes can deliver similar energy density, which translates to the same driving range. As expected, the cell energy density dropped when shorter charging times were used. However, the cells using the LiFSI electrolyte performed much better than cells with the $LiPF_6$ electrolyte. The pouch cells with the former electrolyte could deliver 184.66 Wh/kg energy density when charged in 12-minutes and maintain 161.78 Wh/kg after 500 fast charge cycles. The latter only had 160.37 Wh/kg energy density with 132.76 Wh/kg left after 500 cycles, which further suggests LiFSI is a better Li salt for fast charging Li-ion cells compared to $LiPF_6$.

4. Conclusion

The fast charging performance of high-energy density (NMC811/graphite) Li-ion cells was studied when different lithium salts were used in the electrolyte. LiFSI showed both higher ionic conductivity and Li-ion transference number compared to $LiPF_6$. During a 12-minute fast charging step, cells with $LiPF_6$ electrolyte reached the cut-off voltage in 4.2 min, which is much earlier compared to 7.4 min for LiFSI. LiFSI electrolyte showed 13% capacity improvement in the first cycle of the 12-minute charge. The capacity retention was also significantly higher at 87.7% after 500 cycles with less lithium plating observed. This study shows LiFSI salt can be used for fast charging of Li-ion cells due to its high conductivity, high Li ion transference number and good electrochemical performance.

Acknowledgement

This research at Oak Ridge National Laboratory, managed by UT Battelle, LLC, for the U.S. Department of Energy (DOE) under contract DE-AC05-00OR22725, was sponsored by the Laboratory Directed Research and Development Program and by the Office of Energy Efficiency and Renewable Energy (EERE) Vehicle Technologies Office (VTO) (Technology Manager: Brian Cunningham).

Appendix A. Supplementary data

Supplementary data to this article can be found online at https://doi.org/10.1016/j.elecom.2019.04.013.

References

[1] Z.A. Needell, J. McNerney, M.T. Chang, J.E. Trancik, Potential for widespread electrification of personal vehicle travel in the United States, Nat. Energy 1 (2016), https://doi.org/10.1038/nenergy.2016.112.
[2] D. Howell, S. Boyd, B. Cunningham, S. Gillard, L. Slezak, S. Ahmed, I. Bloom, A. Burnham, K. Hardy, A.N. Jansen, P.A. Nelson, D.C. Robertson, T. Stephens, R. Vijayagopal, R.B. Carlson, F. Dias, E.J. Dufek, C.J. Michelbacher, M. Mohanpurkar, D. Scoffield, M. Shirk, T. Tanim, M. Keyser, C. Kreuzer, O. Li, A. Markel, A. Meintz, A. Pesaran, S. Santhanagopalan, K. Smith, E. Wood, J. Zhang, Enabling fast charging: enabling fast charging: a technology gap assessment, (2017) https://energy.gov/sites/prod/files/2017/10/f38/XFC Technology Gap Assessment Report_FINAL_10202017.pdf.
[3] Z. Du, D.L. Wood, C. Daniel, S. Kalnaus, J. Li, Understanding limiting factors in thick electrode performance as applied to high energy density Li-ion batteries, J. Appl. Electrochem. 47 (2017) 405–415, https://doi.org/10.1007/s10800-017-1047-4.
[4] K.G. Gallagher, S.E. Trask, C. Bauer, T. Woehrle, S.F. Lux, M. Tschech, P. Lamp, B.J. Polzin, S. Ha, B. Long, Q. Wu, W. Lu, D.W. Dees, A.N. Jansen, Optimizing areal capacities through understanding the limitations of lithium-ion electrodes, J. Electrochem. Soc. 163 (2016) A138–A149, https://doi.org/10.1149/2.0321602jes.
[5] S. Ahmed, I. Bloom, A.N. Jansen, T. Tanim, E.J. Dufek, A. Pesaran, A. Burnham, R.B. Carlson, F. Dias, K. Hardy, M. Keyser, C. Kreuzer, A. Markel, A. Meintz, C. Michelbacher, M. Mohanpurkar, P. Nelson, D.C. Robertson, D. Scoffield, M. Shirk, T. Stephens, R. Vijayagopal, J. Zhang, Enabling fast charging – a battery technology gap assessment, J. Power Sources 367 (2017) 250–262, https://doi.org/10.1016/j.jpowsour.2017.06.055.
[6] Z. Li, J. Huang, B. Yann Liaw, V. Metzler, J. Zhang, A review of lithium deposition in lithium-ion and lithium metal secondary batteries, J. Power Sources 254 (2014) 168–182, https://doi.org/10.1016/j.jpowsour.2013.12.099.
[7] M. Broussely, P. Biensan, F. Bonhomme, P. Blanchard, S. Herreyre, K. Nechev, R.J. Staniewicz, Main aging mechanisms in Li ion batteries, J. Power Sources (2005) 90–96, https://doi.org/10.1016/j.jpowsour.2005.03.172.
[8] J.N. Chazalviel, Electrochemical aspects of the generation of ramified metallic electrodeposits, Phys. Rev. A 42 (1990) 7355–7367, https://doi.org/10.1103/PhysRevA.42.7355.
[9] H.J. Chang, A.J. Ilott, N.M. Trease, M. Mohammadi, A. Jerschow, C.P. Grey, Correlating microstructural lithium metal growth with electrolyte salt depletion in lithium batteries using 7Li MRI, J. Am. Chem. Soc. 137 (2015) 15209–15216, https://doi.org/10.1021/jacs.5b09385.
[10] J.H. Cheng, A.A. Assegie, C.J. Huang, M.H. Lin, A.M. Tripathi, C.C. Wang, M.T. Tang, Y.F. Song, W.N. Su, B.J. Hwang, Visualization of lithium plating and stripping via in operando transmission X-ray microscopy, J. Phys. Chem. C 121 (2017) 7761–7766, https://doi.org/10.1021/acs.jpcc.7b01414.

[11] F. Orsini, A.D. Pasquier, B. Beaudoin, J. Tarascon, M. Trentin, N. Langenhuizen, E. De Beer, P. Notten, In situ Scanning Electron Microscopy (SEM) observation of interfaces within plastic lithium batteries, J. Power Sources 76 (1998) 19–29, https://doi.org/10.1016/S0378-7753(98)00128-1.

[12] L. Li, S. Zhou, H. Han, H. Li, J. Nie, M. Armand, Z. Zhou, X. Huang, Transport and electrochemical properties and spectral features of non-aqueous electrolytes containing LiFSI in linear carbonate solvents, J. Electrochem. Soc. 158 (2010) A74, https://doi.org/10.1149/1.3514705.

[13] H.B. Han, S.S. Zhou, D.J. Zhang, S.W. Feng, L.F. Li, K. Liu, W.F. Feng, J. Nie, H. Li, X.J. Huang, M. Armand, Z. Bin Zhou, Lithium bis(fluorosulfonyl)imide (LiFSI) as conducting salt for nonaqueous liquid electrolytes for lithium-ion batteries: physicochemical and electrochemical properties, J. Power Sources 196 (2011) 3623–3632, https://doi.org/10.1016/j.jpowsour.2010.12.040.

[14] Y. Yamada, M. Yaegashi, T. Abe, A. Yamada, A superconcentrated ether electrolyte for fast-charging Li-ion batteries, Chem. Commun. 49 (2013) 11194–11196, https://doi.org/10.1039/c3cc46665e.

[15] S.J. Kang, K. Park, S.H. Park, H. Lee, Unraveling the role of LiFSI electrolyte in the superior performance of graphite anodes for Li-ion batteries, Electrochim. Acta 259 (2018) 949–954, https://doi.org/10.1016/j.electacta.2017.11.018.

[16] S.E. Trask, K.Z. Pupek, J.A. Gilbert, M. Klett, B.J. Polzin, A.N. Jansen, D.P. Abraham, Performance of full cells containing carbonate-based LiFSI electrolytes and silicon-graphite negative electrodes, J. Electrochem. Soc. 163 (2015) A345–A350, https://doi.org/10.1149/2.0981602jes.

[17] D.L. Wood, Z. Du, M. Wood, J. Li, Manufacturing R & D for low-cost, batteries for transportation applications, 34th Annu. Int. Batter. Semin. Exhib, 2017.

[18] J. Zhao, L. Wang, X. He, C. Wan, C. Jiang, Determination of lithium-ion transference numbers in LiPF–PC solutions based on electrochemical, J. Electrochem. Soc. 155 (2008) A292, https://doi.org/10.1149/1.2837832.

[19] S. Zugmann, M. Fleischmann, M. Amereller, R.M. Gschwind, H.D. Wiemhöfer, H.J. Gores, Measurement of transference numbers for lithium ion electrolytes via four different methods, a comparative study, Electrochim. Acta 56 (2011) 3926–3933, https://doi.org/10.1016/j.electacta.2011.02.025.

[20] K. Periyapperuma, T.T. Tran, S. Trussler, D. Ioboni, M.N. Obrovac, Conflat two and three electrode electrochemical cells, J. Electrochem. Soc. 161 (2014), https://doi.org/10.1149/2.0721414jes.

[21] M.S. Ding, K. Xu, S.S. Zhang, K. Amine, G.L. Henriksen, T.R. Jow, Change of conductivity with salt content, solvent composition, and temperature for electrolytes of LiPF[sub 6] in ethylene carbonate-ethyl methyl carbonate, J. Electrochem. Soc. 148 (2001) A1196, https://doi.org/10.1149/1.1403730.

[22] H.B. Han, S.S. Zhou, D.J. Zhang, S.W. Feng, L.F. Li, K. Liu, W.F. Feng, J. Nie, H. Li, X.J. Huang, M. Armand, Z.B. Zhou, Lithium bis(fluorosulfonyl)imide (LiFSI) as conducting salt for nonaqueous liquid electrolytes for lithium-ion batteries: physicochemical and electrochemical properties, J. Power Sources (2011), https://doi.org/10.1016/j.jpowsour.2010.12.040.

[23] J. Evans, C.A. Vincent, P.G. Bruce, Electrochemical measurement of transference numbers in polymer electrolytes, Polymer (Guildf) 28 (1987) 2324–2328, https://doi.org/10.1016/0032-3861(87)90394-6.

[24] P. Nelson, K. Gallagher, I. Bloom, D. Dees, S. Ahmed, BatPaC (battery performance and cost) software, Argonne Natl. Lab. [Online]. Available http://www.cse.anl.gov/BatPaC/. (n.d.).